Integrating Spatial Analyses and Microbotanical Remains: A Methodological Approach for Investigating Plant Processing Activities and Domestic Spaces at Neolithic Çatalhöyük.

Carlos G. Santiago-Marrero [a] [b] *, Carla Lancelotti [b] [c] and Marco Madella [b] [c].

[a] HUMANE—Human Ecology and Archaeology, IMF, CSIC, 08001, Barcelona, Spain.

[b] CASEs Research Group, Department of Humanities, Universitat Pompeu Fabra, Barcelona, Spain.

[c] ICREA - Passeig Lluís Companys 23, 08010 Barcelona, Spain.

Supplementary II

1.0 Detailed description of starch grain typologies and reference material

Type 1 – medium to large size, round or slightly oval in 2D and lenticular in 3D, centric hilum and present a distinct centric cross (x) with straight arms. Fissures are not common, and present distinct centric lamellae forming rings, and some grains present distinctive pressure facets resembling craters ("golf ball-like"). Starch grains with these characteristics commonly occur in the Triticeae tribe and are referred to in the literature as Triticeae A-type (Cristiani et al., 2016; Geera et al., 2006; Yang et al., 2012; Yang and Perry, 2013).

Type 2 – medium size, polygonal to sub-round shaped in 2D and polyhedral in 3D. It has a centric open hilum and an extinction cross (x) with straight arms (Figure S1. A-B). Fissures are occasionally visible at the hilum in the form of a central depression or lineal and Y-shaped fissures. Lamellae are not visible, and grains present angular pressure facets. Starch grains with these characteristics are common in small-seeded taxa of the Panicoideae sub-family (Liu et al., 2014a, 2014b; Lucarini and Radini, 2020; Madella et al., 2016; Yang et al., 2012) (Figure S1. C-D).

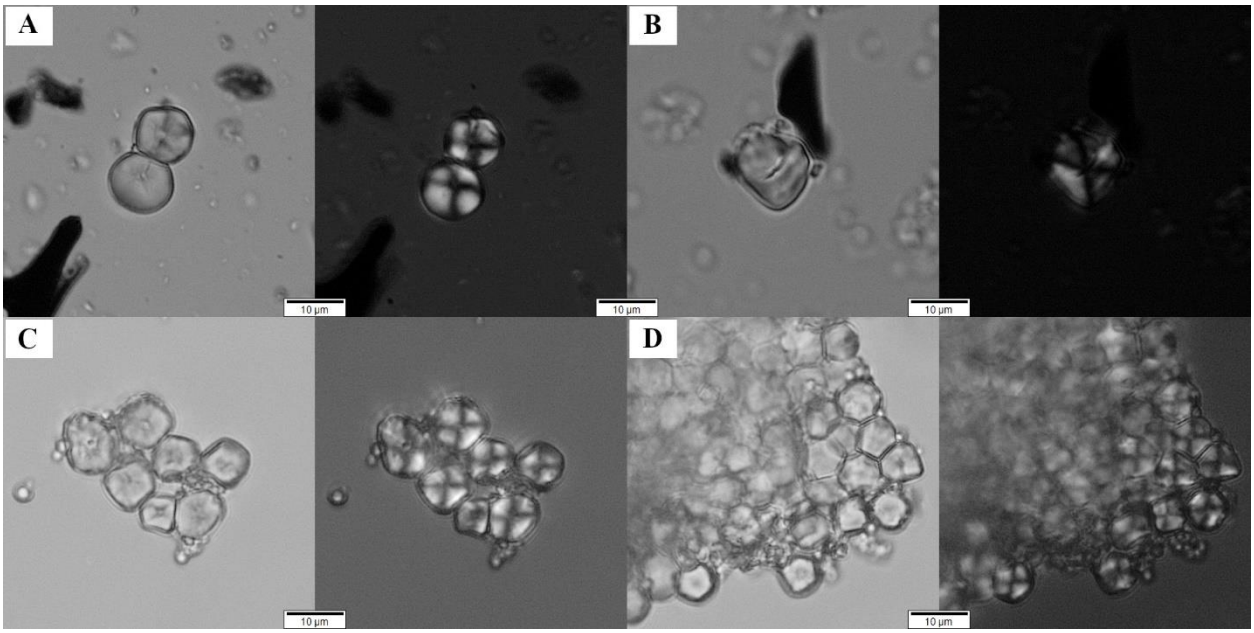

Figure S1. Archaeological (**A-B**) and modern starch grains (**C-D**) from caryopses of small-seeded taxa of the Panicoideae sub-family under brightfield (left) and cross-polarised (right) light at 400x magnification: **A.** Starch grains Type 2 recovered from Building 80; **B.** Single starch grain Type 2 recovered from Building 131; **C-D.** Starch grains from *Setaria verticillata* (L.).

Type 3 – medium to large size, bimodal in 2D presenting oval irregular shapes, and reniform in 3D. The hilum is open and irregular, and the extinction cross (x) can be asymmetric in some cases. It is common to see a cleft or deep longitudinal fissure in the centric area splitting the grain into two or more fragments, and the lamellae present continuous rings. Starch grains with these characteristics are commonly found in the Faboideae sub-family (Henry et al., 2009; Pagán-Jiménez, 2015).

Type 4 – large size, oval to oval-elongated in 2D and cylindrical to ovoid in 3D. It has an eccentric hilum and presents an extinction cross (x) with curved elongated arms. The lamellae are visible forming eccentric bands, and no other features such as fissures and pressure facets are visible. Based on the reference collection and in accordance with the literature, these characteristics are consistent with starch grains produced by different geophyte taxa, cf. Liliaceae/Iridaceae (Liu et al., 2019) (Figure S2).

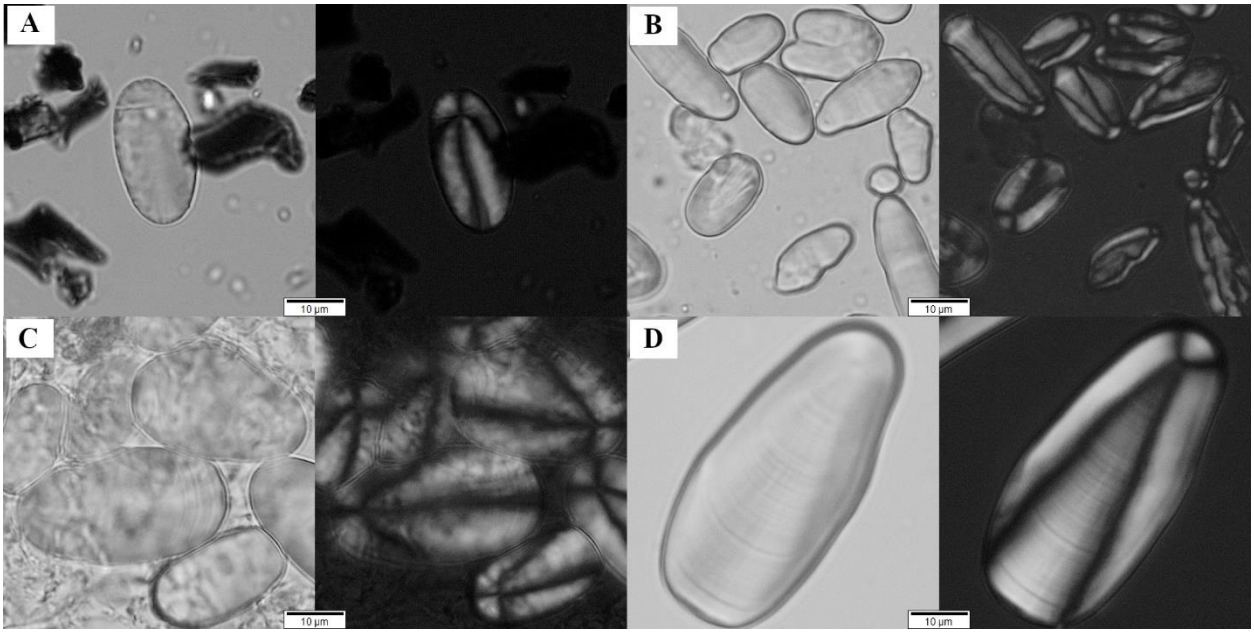

Figure S2. Archaeological (**A**) and modern starch grains (**B-D**) from underground storage organs of Iridaceae and Liliaceae geophytes under brightfield (left) and cross-polarised (right) light at 400x magnification: **A.** Starch grain Type 4 recovered from Building 80; **B.** Starch grain from the USO of *Iris* sp.; **C.** Starch grains from the USO of *Lilium martagon* L.; **D.** Starch grain from the USO of *Lilium candidum* L.

Type 5 – small to large size, bi-modal, exhibiting semi-polygonal expanded to oval-truncated in 2D and semi-ovoid in 3D. It has a centric open hilum, and the extinction cross can present "x" to "+" shapes with straight and wide arms. It presents a central depression in the hilum, and visible lamellae forming coarse concentric rings. However, examples from Building 131 do not present the coarse lamellae rings which may be indicative of different taphonomic processes occurring at each building. No evident pressure facets are observed, but the oval truncated morphotypes (oval with one slightly angular side) may be caused while growing tightly or attached to other starch grains in the amyloplast. The taxonomic origin of this type remains indeterminate.

Type 6 – medium size, elongated plano-convex (bell shape) in 2D and parabolic prism (elliptical cone) in 3D. It presents an eccentric (but close to the mesial area) hilum and extinction cross (x) with occasionally wavy arms. This type presents a variance with short and U-shaped specimens and with two distal flat bases or pressure facets. The taxonomic or organ origin of this type remains unidentified.

Type 7 – small to large size, trapezoidal elongated in 2D and semi-oval to prismatic in 3D. It has an eccentric hilum (but sometimes centric) and the extinction cross (x) is visible, presenting straight arms with an occasional z-shape toward the starch margin. Some starch grains present a Y-shape or radial fissure, the lamellae are not visible and some occasional angular pressure facets were observed. Starch grains with these characteristics resemble morphologies found in big seeded taxa of the Panicoideae sub-family and it has been classified as such by some researchers (Cristiani et al., 2021; Liu et al., 2018a; Yang et al., 2016). However, starch grains from this sub-family present centric hilum and extinction cross (Madella et al., 2016; Yang et al., 2012), and similar morphotypes have been observed in geophyte taxa (e.g., Sugiyama et al., 2022), therefore its taxonomic origin is not clear yet.

Type 8 – small size, circular to oval in 2D and spherical to ovoid in 3D. It has a centric hilum occasionally visible and an extinction cross (x) occasionally faint with straight arms. No apparent fissures are present, but some grains present radial lines in the hilum. No lamellae nor pressure facets were observed. This type could represent transient starch grains which are synthesised within the chloroplast in the plant leaves during the day forming indeterminate shapes less than 7μm in size, being degraded and metabolised quickly during the night when photosynthesis cannot continue (Gott et al., 2006; Haslam, 2004; Pfister and Zeeman, 2016). However, starch grains with these characteristics can be found in many Triticeae taxa as well (e.g., *T. timopheevii, T. dicoccum, T. monococcum, T. aestivum* L.) forming aggregates with Triticeae A-type, where is known as B-type (≤10 μm) (Ao and Jane, 2007; Barton et al., 2018; Geera et al., 2006) (Figure S3. A). However, based on some examples of Type 8 attached to Type 5 it is probable that other small redundant forms of young and/or transient starch grains from undetermined species may be

represented, presenting indirect evidence for a non-Triticeae origin for Type 8, or at least for some of them (Figure S3. B-C).

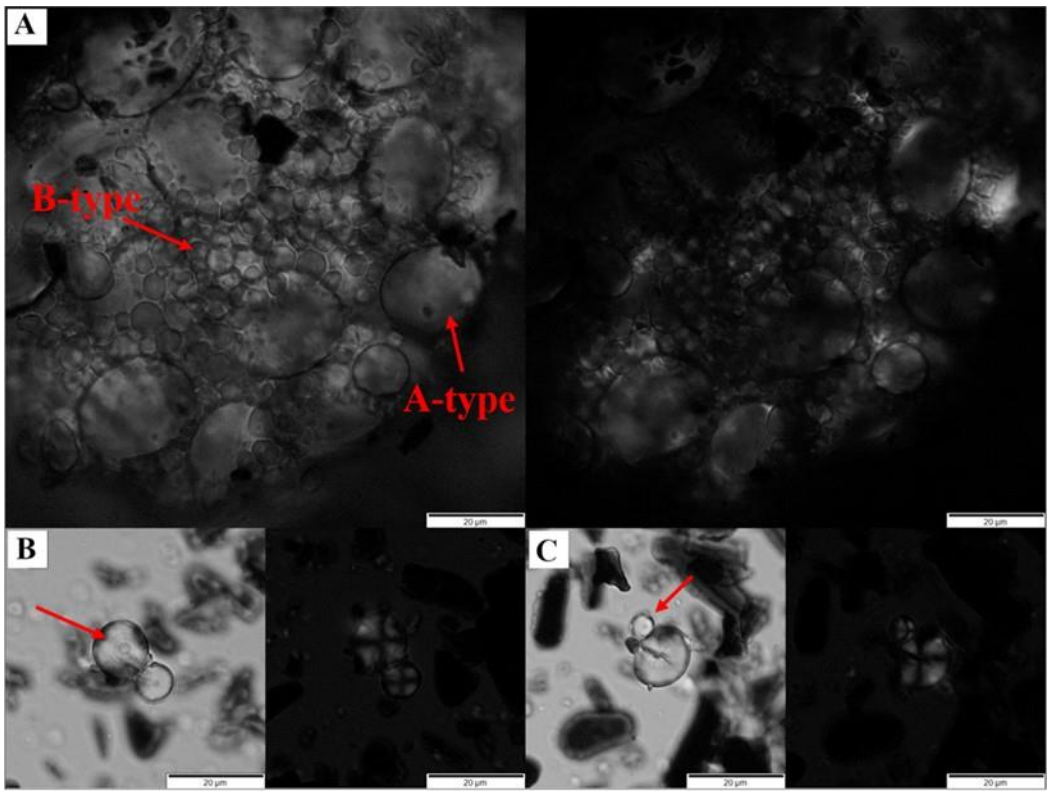

Figure S3. Archaeological starch grains recovered from Building 80 under brightfield (left) and cross-polarized (right) light at 400x magnification: **A**. Bimodal aggregate of Triticeae A-type (Type 1), notice the dimple (golf ball-like) pressure facets pointed by the red arrow, and B-type starch grains ≤ 10μm in size (Type 8); **B**. Example of Type 5 starch grain (large) coupled to small (≤ 10 μm) young or transient starch sharing characteristics with Type 8, the red arrow points to the characteristic coarse lamellae and open hilum of Type 5. **C.** Another example of Type 5 and a young or transient starch grain sharing characteristics with Type 8, pointed by the red arrow.

Type 9 – medium to large size, sub-triangular in 2D and parabolic in 3D. It has an open and centric hilum and an extinction cross in (x) with curved or slightly bent arms becoming diffused toward the starch margin. Visible lamellae reproducing the starch grain geometric shape (semi-triangular) instead of presenting concentric or curved rings or bands (Figure S4. A-B). In the case of Building

131, Type 9 is rather large sized and presents a faint line or crease departing from the hilum and extending toward the distal margins and presenting a straight pressure facet on the distal margin probably caused while growing attached to other starch grains. Based on the reference collection and following the literature, these characteristics are consistent with starch grains produced by different geophyte taxa (Ahituv and Henry, 2022; Henry, 2020; Liu et al., 2020, 2013; Mercader et al., 2018) cf. Iridaceae/Araceae (Figure S4. C-F).

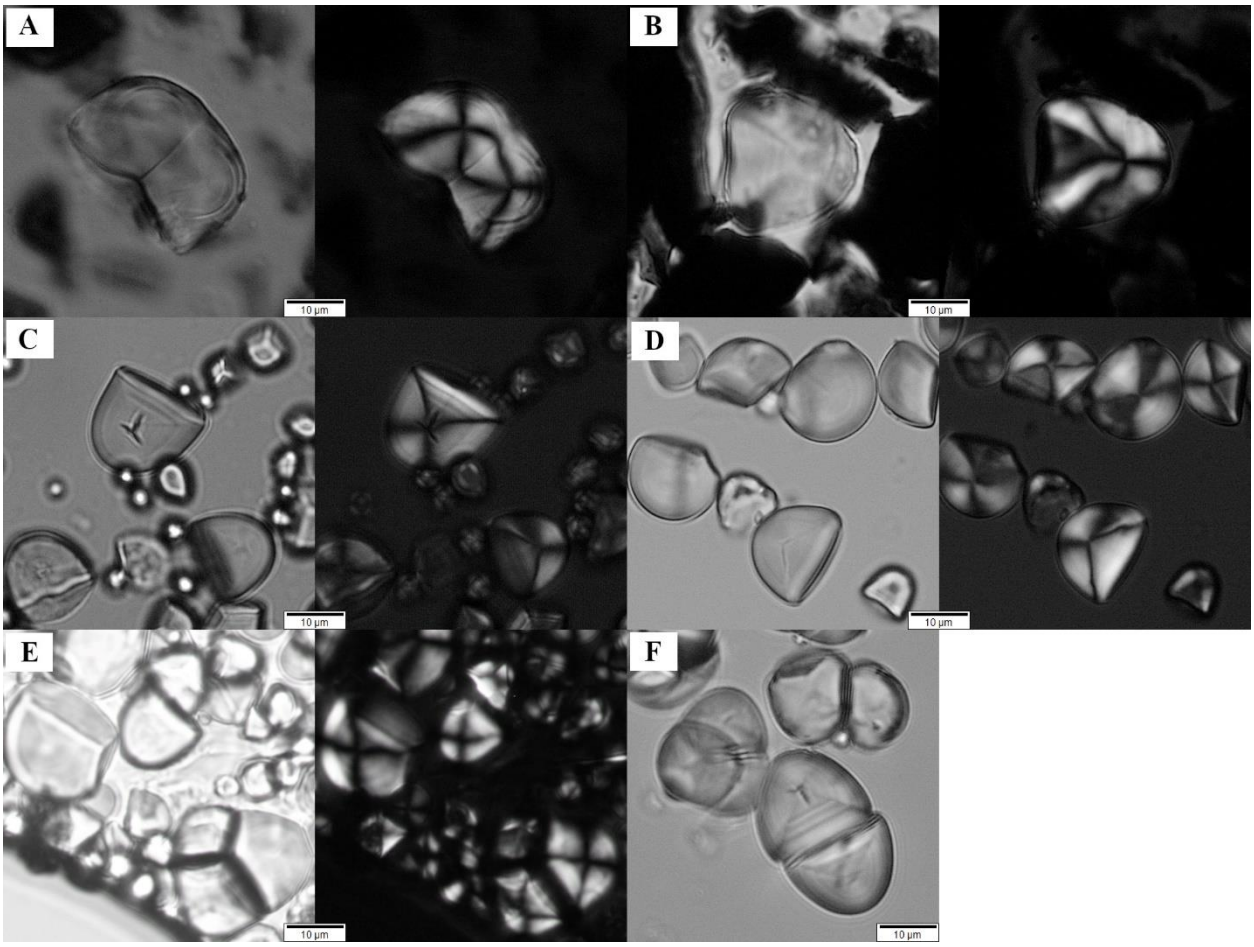

Figure S4. Archaeological (**A-B**) and modern starch grains (**C-F**) from underground storage organs of Iridaceae and Araceae geophytes under brightfield (left) and cross-polarised (right) light at 400x magnification: **A.** Starch grains Type 9 slightly gelatinised recovered from Building 80; **B.** Starch grain Type 9 recovered from Building 131; **C.** Starch grains from the USO of *Crocus sativus* L.; **D.** Starch grain from the USO of Araceae sp.; **E-F.** Starch grain from the USO of *Arisarum vulgare* O.Targ.Tozz.

Type 10 – small to medium size, oval to circular in 2D and ovoid in 3D. It has a centric hilum and extinction cross (x) with straight to curved arms and a centric "Y" or radial shape fissure in the hilum. Occasionally visible lamellae in some grains, although incomplete. No pressure facets were observed. This type occasionally occurs in an irregular form, but it is not clear if this is due to some sort of taphonomic process. While at the moment the taxonomic origin of this type is not clear, previous studies at the site identified this type as originating from helophyte taxa such as Cyperaceae and Typhaceae (Santiago-Marrero et al., 2021).

Type 11 – small to medium size, this bimodal type occurs as triangular or trapezoidal in 2D and polyhedral in 3D. The hilum is centric and the extinction cross (x) is visible with slightly bent arms and no visible lamellae. Some starch grains present central creases, radial lines, or fissures, and angular pressure facets are observed, caused by the grains being attached into small clumps of aggregated starch. This type may be redundant when presented as single grains. However, when found as aggregates, their taxonomic value increases, being traceable to various genera within the Pooideae sub-family such as *Avena* (Ahituv and Henry, 2022; Cagnato et al., 2021; Henry, 2020; Lentfer, 2009; Liu et al., 2020) (Figure S5).

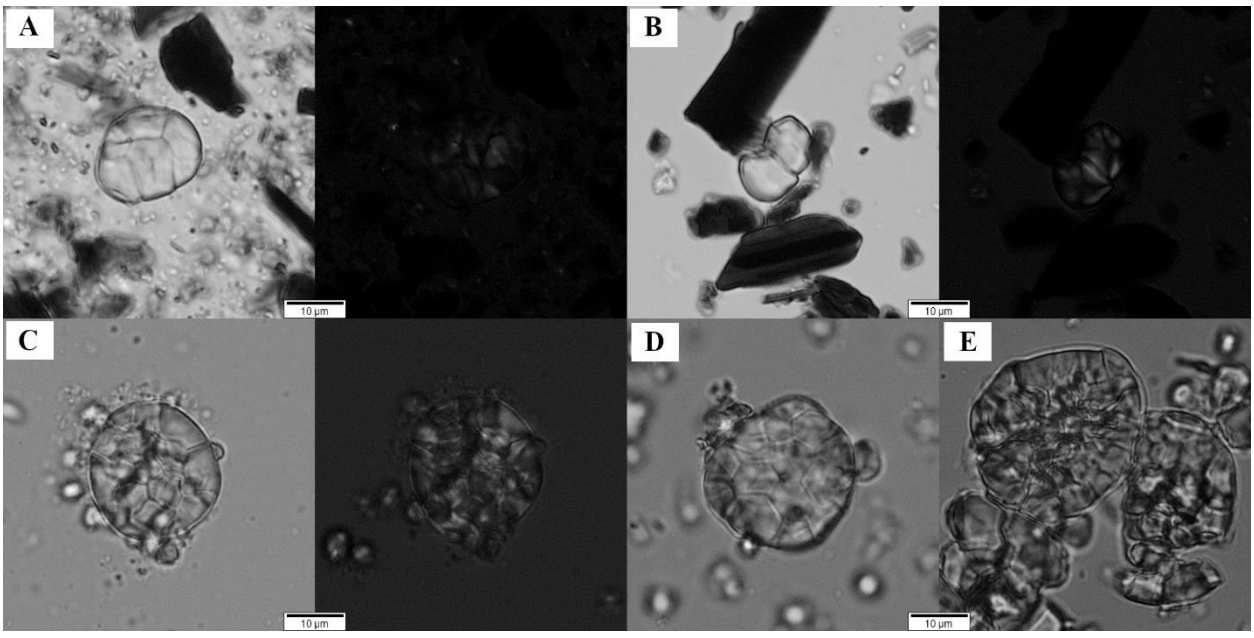

Figure S5. Archaeological (**A-B**) and modern starch grains (**C-E**) from the caryopses of *Avena* under brightfield (left) and cross-polarised (right) light at 400x magnification: **A.** Aggregate of starch grain Type 11 recovered from Building 80; **B.** Starch grains Type 11 recovered from Building 131; **C.** Aggregate of starch grain from *Avena barbata* Pott ex Link.; **D.** Aggregate of starch grain from *Avena byzantina* K.Koch; **E.** Aggregate of starch grain from *Avena sativa* L.

Type 12 – medium to large size, polygonal to sub-round shaped in 2D and polyhedral in 3D. It has a centric hilum and an extinction cross (x) with straight arms. Fissures are occasionally visible at the hilum in the form of a central depression or lineal or Y-shaped crack and present angular margins. Lamellae are not visible, and the grains present angular pressure facets. Starch grains with these characteristics are commonly associated with the big seeded taxa from the Panicoideae sub-family (García-Granero et al., 2018; Liu et al., 2018b; Lucarini et al., 2016) (Figure S6).

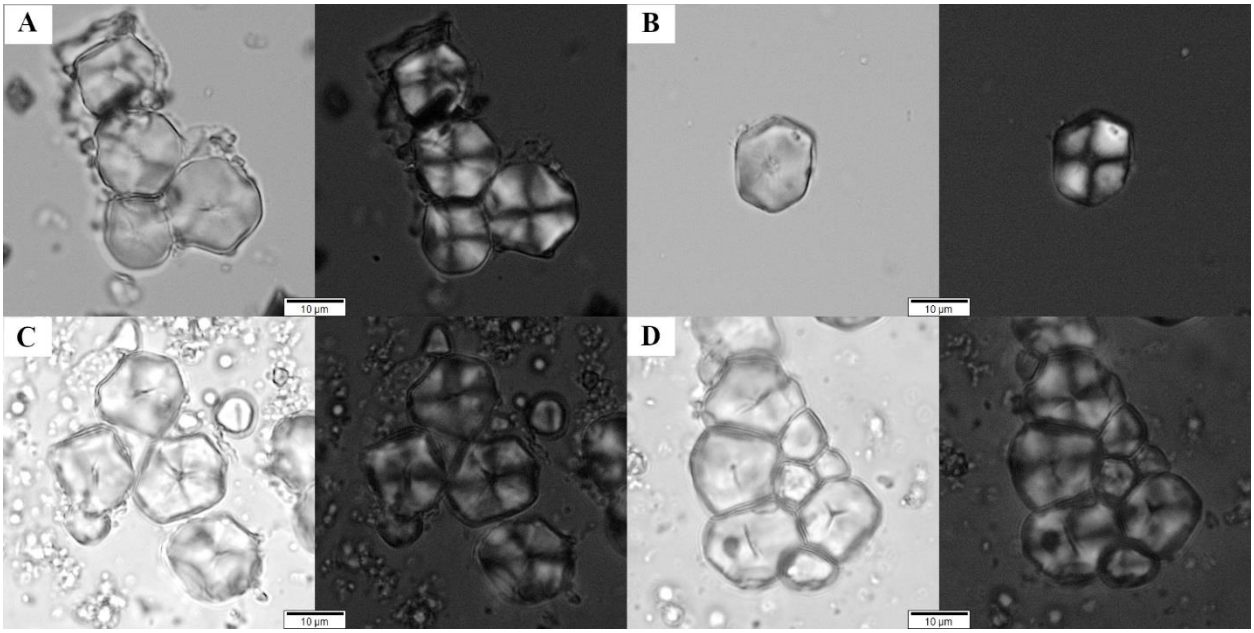

Figure S6. Archaeological (**A-B**) and modern starch grains (**C-D**) from caryopses of big-seeded taxa from the Panicoideae sub-family under brightfield (left) and cross-polarised (right) light at 400x magnification: **A.** Starch grains Type 12 recovered from Building 80; **B.** Single starch grain Type 12 recovered from Building 131; **C-D.** Starch grains from *Sorghum halepense* (L.) Pers.

Type 13 – large size, semi-circular in 2D and ovoid in 3D. It has an eccentric open hilum and presents a distinctive eccentric extinction cross (x) with curved to wavy elongated arms. Some grains present an occasional longitudinal fissure, but these may be caused by taphonomy. The lamellae are arranged as rounded eccentric elliptical rings and bands. These characteristics are consistent with starch grains produced by different geophyte taxa (Pagán-Jiménez, 2015; Wang et al., 2017).

Type 14 – large size, elongated with round proximal and slightly flattened distal edges in 2D and cylindrical in 3D. It has an eccentric hilum and presents an eccentric extinction cross (x) with undulated elongated arms. It has a distinct lamella visible throughout the starch surface producing rounded bands that turn more angular echoing the distal edge upon approaching it. In the case of Building 131, Type 14 is medium size and has a slightly conoid 3D shape. These characteristics are consistent with starch grains produced by different geophyte taxa, cf. Liliaceae/Iridaceae (Liu et al., 2018b; Pagán-Jiménez, 2015).

Type 15 – large size, triangular elongated in 2D and parabolic prism (elliptical cone) in 3D with rounded proximal and slightly flattened distal edges. It has a visible eccentric hilum and extinction cross (x) with elongated arms. However, these are not completely visible due to the attached particles. There are no apparent fissures, and the lamellae form continuous and homogeneous bands. These characteristics are consistent with starch grains produced by different geophyte taxa, cf. Liliaceae/Iridaceae (Pagán-Jiménez, 2015; Wang et al., 2019)**.**

Type 16 – large size, oval in 2D and ellipsoid or reniform in 3D. It has an eccentric hilum and eccentric extinction cross (x) with elongated curved to wavy arms and the lamellae forming concentric rings. Longitudinal fissures are occasionally visible, but these seem to originate from taphonomy. No pressure facets are present. These characteristics are consistent with starch grains produced by different geophyte taxa (Pagán-Jiménez, 2015).

Type 17 – medium to large size, circular to oval in 2D and ovoid in 3D. The hilum is eccentric, visible, and occasionally open, and presents an eccentric extinction cross (x) with straight or wavy elongated arms. Some grains present a longitudinal or radial fissure in the hilum, but these may originate from taphonomy. The lamellae form eccentric concentric rings, and no pressure facets are present. These characteristics are consistent with starch grains produced by different geophyte taxa (Liu et al., 2019, 2014a, 2013; Yang et al., 2016; Zhang et al., 2017).

Type 18 – large size, triangular or petaloid in 2D with rounded proximal and slightly flattened distal ends and occasionally reniform in 3D. The hilum is eccentric and open, and the extinction cross (x) presents curved to wavy elongated arms. Some fissures may be observed in the hilum, probably caused by taphonomy. The lamellae present continuous parabolic shape rigs and bands increasing towards the distal end. These characteristics are consistent with starch grains produced by different geophyte taxa, cf. Liliaceae/Iridaceae (Liu, 2015; Liu et al., 2015, 2014a; Mercader et al., 2018; Pagán-Jiménez, 2015; Zhang et al., 2021).

Type 19 – large size, irregular-conoid with a wide rounded proximal and a narrow distal end, it was not possible to record its 3D form. The hilum is visible and eccentrically located towards the wider end and the extinction cross (x) is eccentric with wavy elongated arms. The grain presents radial fissures and clefts, probably caused by mechanical pressure. It has faint lamellae, but when visible, they produce concentric rings around the hilum and parabolic shape bands towards the distal end. These characteristics are consistent with starch grains produced by different geophyte taxa (Liu et al., 2018a; Pagán-Jiménez, 2015; Wang et al., 2019).

Type 20 – medium to large size, big oval to triangular in 2D and guttiform in 3D. The hilum can be centric or eccentric and produces an extinction cross (x) with straight or curved arms. It has a central longitudinal crease or cleft. It has faint lamellae, but when visible, they produce concentric rings. No pressure facets were observed. Based on the literature, this type shares descriptive and

metric similarities with starch grains produced by *Quercus* spp. (Cagnato et al., 2021; Guan et al., 2014; Tsafou and García-Granero, 2021; Wang et al., 2021, 2019; Wang and Jiang, 2021a, 2021b; Yao et al., 2016).

Type 21 – large size, oval in 2D and ellipsoid in 3D. The hilum is eccentric and visible and exhibits an eccentric extinction cross (x) with curved and diffused arms. Fissures are not apparent but present longitudinal creases extending from the hilum to the distal end. The lamellae can be observed through all the starch grain surfaces forming regular elliptical bands and no pressure facets are visible. These characteristics are consistent with starch grains produced by different geophyte taxa (Tsafou and García-Granero, 2021).

No type – this group contains three major types of starch grains: (1) starch grains lacking well-defined diagnostic features such as simple spherical or oval starch grains with straight "+ or x" arms; (2) starch in agglomeration with other particles or micro-charcoal obstructing a full observation of the starch dimensions, morphology, or features; and (3) Starch grains sharing similar morphologies but presenting different features like hilum fissures for example (Figure S7. A-D). While some of these characteristics may hold diagnostic value, they could also be produced by taphonomic processes such as mechanical pressure (Mickleburgh and Pagán-Jiménez, 2012). Therefore, due to the lack of published information or reference material to compare with, and in recognition of the complexity of the archaeological context and the different taphonomic processes starches may have been exposed to, these grains were added to this category.

Damaged – in this group were binned all starch grains with different levels of structural damage such as pressure, gelatinisation, or enzymatic action, including broken starch grains or fragments (Figure S7. E-F). The damage prevented a secure description and classification -or taxonomic identification- of the recorded starch. The most prominent damage was recorded, but no further interpretations were made. The reason for this is that starch grains preserved sediments could have been exposed to microbial activity and unknown taphonomic processes (Dubreuil et al., 2015;

Torrence, 2006). Therefore, due to the complexity of these post-depositional processes, no secured conclusion could be achieved from taphonomic observations in starch grains in this case.

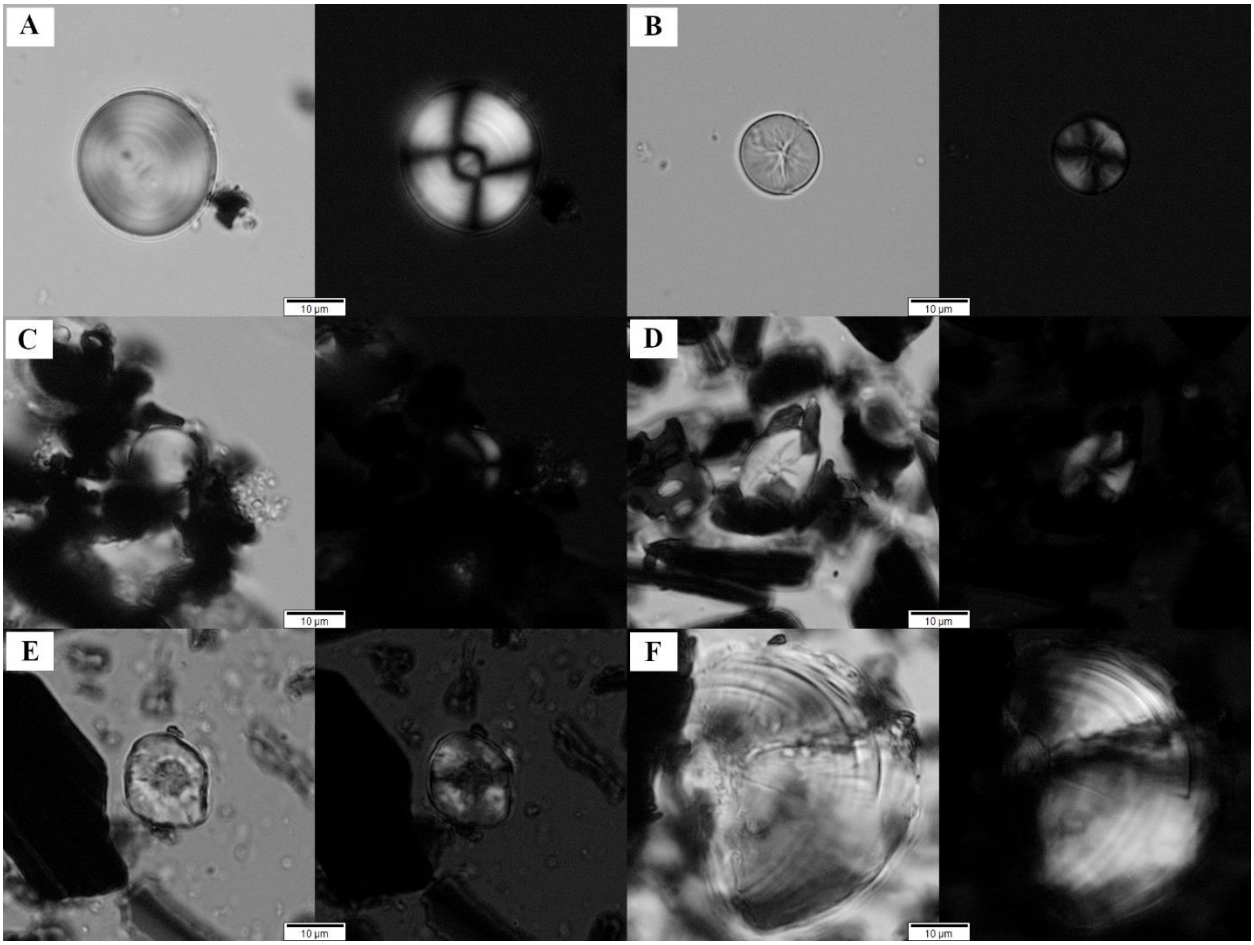

Figure S7. Archaeological starch grains recovered from Building 131 under brightfield (left) and cross-polarised (right) light at 400x magnification: **A.** Taxonomically indeterminate half-compound starch with two visible open hila and a set of lamellae; **B.** Taxonomically indeterminate starch grain presenting radial lines and radial fissures; **C-D.** Examples of starch grains trapped within charcoal particles obstructing its full recording; **E**. Starch grain presenting enzymatic damage; **F**. Broken USO starch grain presenting evidence for gelatinization and pressure damage.

2.0 Examples of phytoliths morphotypes identified in Building 80 and 131

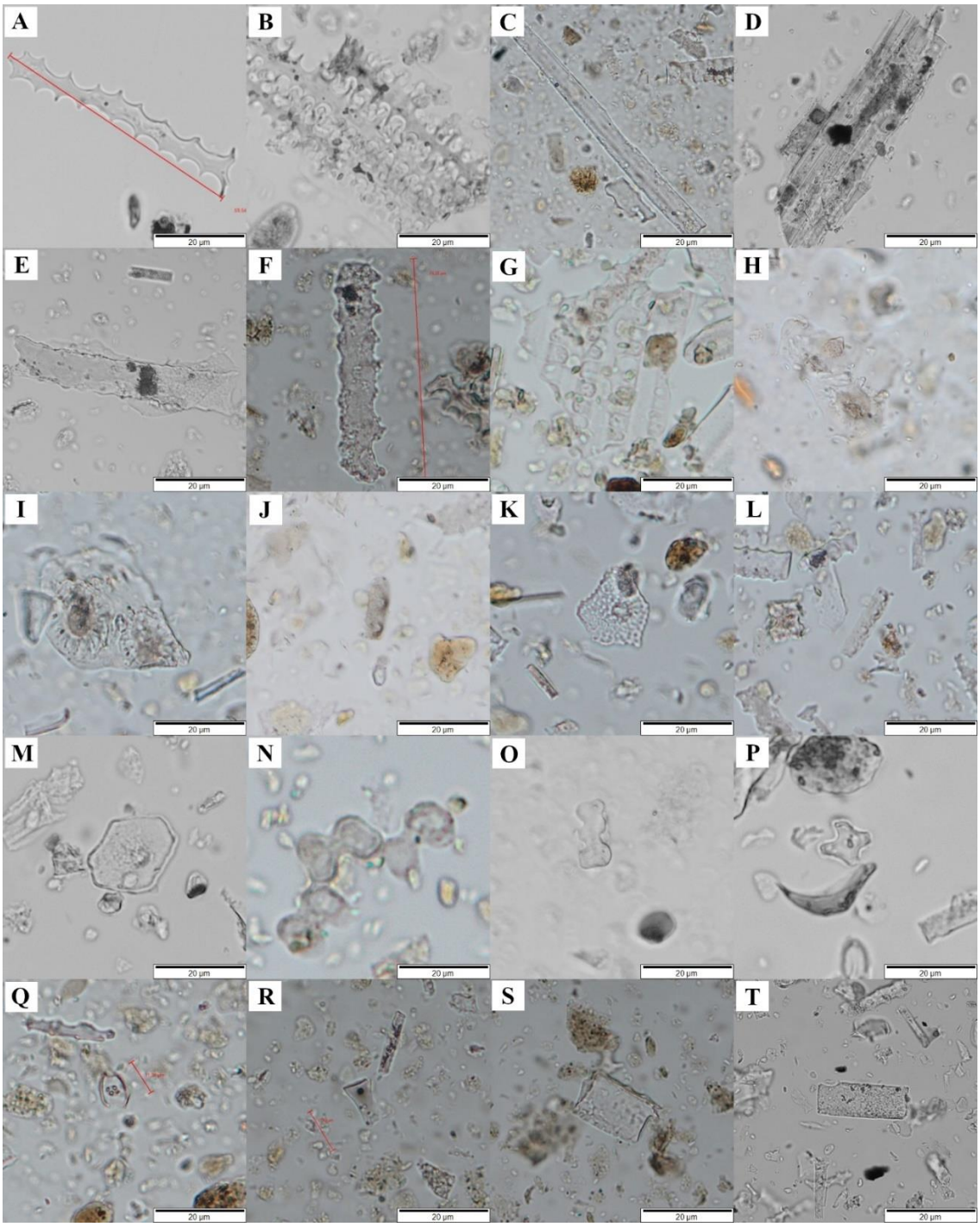

Figure S8. Phytolith morphotypes at 400x magnification: **A)** Elongate echinate; **B)** Elongate dendritics in anatomical connection; **C)** Elongate psilate; **D)** Elongate psilates in anatomical connection; **E-F)** Elongate irregular; **G)** Elongate columellate (∩) in anatomical connection; **H-I)**

papillae; **J-M)** Cyperaceae papillae; **N)** Bilobate; **O)** Polylobate; **P)** Cross; **Q)** Saddle; **R)** Rondel; **S-T)** Rectangular/Tabular.

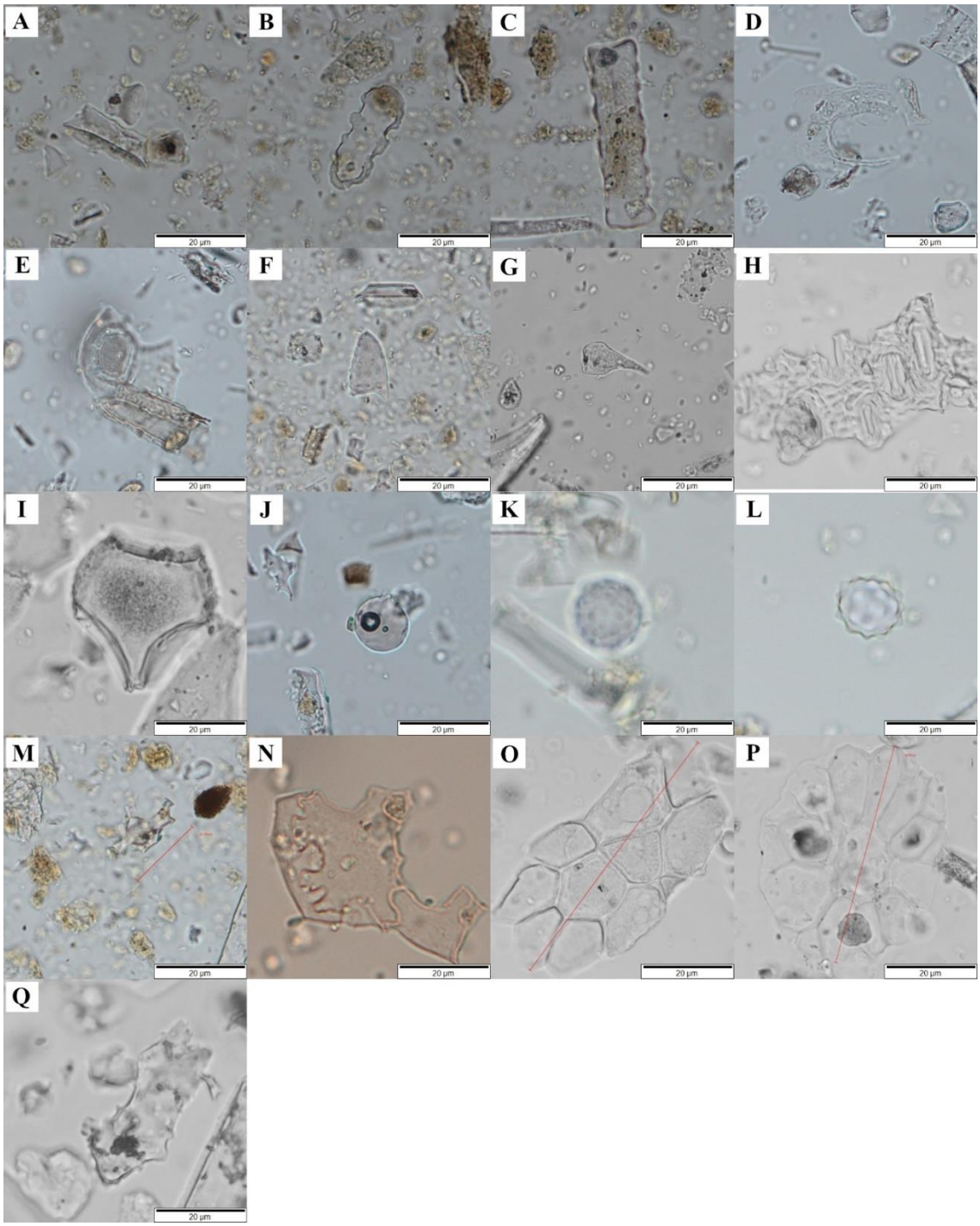

Figure S9. Phytolith morphotypes at 400x magnification: **A)** Trapeziforms **B)**; Trapeziform polylobate; **C)** Trapeziform sinuate; **D-E)** Silicified trichome bases; **F-G)** Trichomes; **H)** Stomas;

I) Bulliform cuneiform; **J)** Globular psilate; **K)** Globular granulate; **L)** Globular echinate; **M)** Polyhedral; **N)** Jigsaw; **O-P)** Polygonal; **Q)** Amoeboid.

3.0 Ordinary kriging variograms

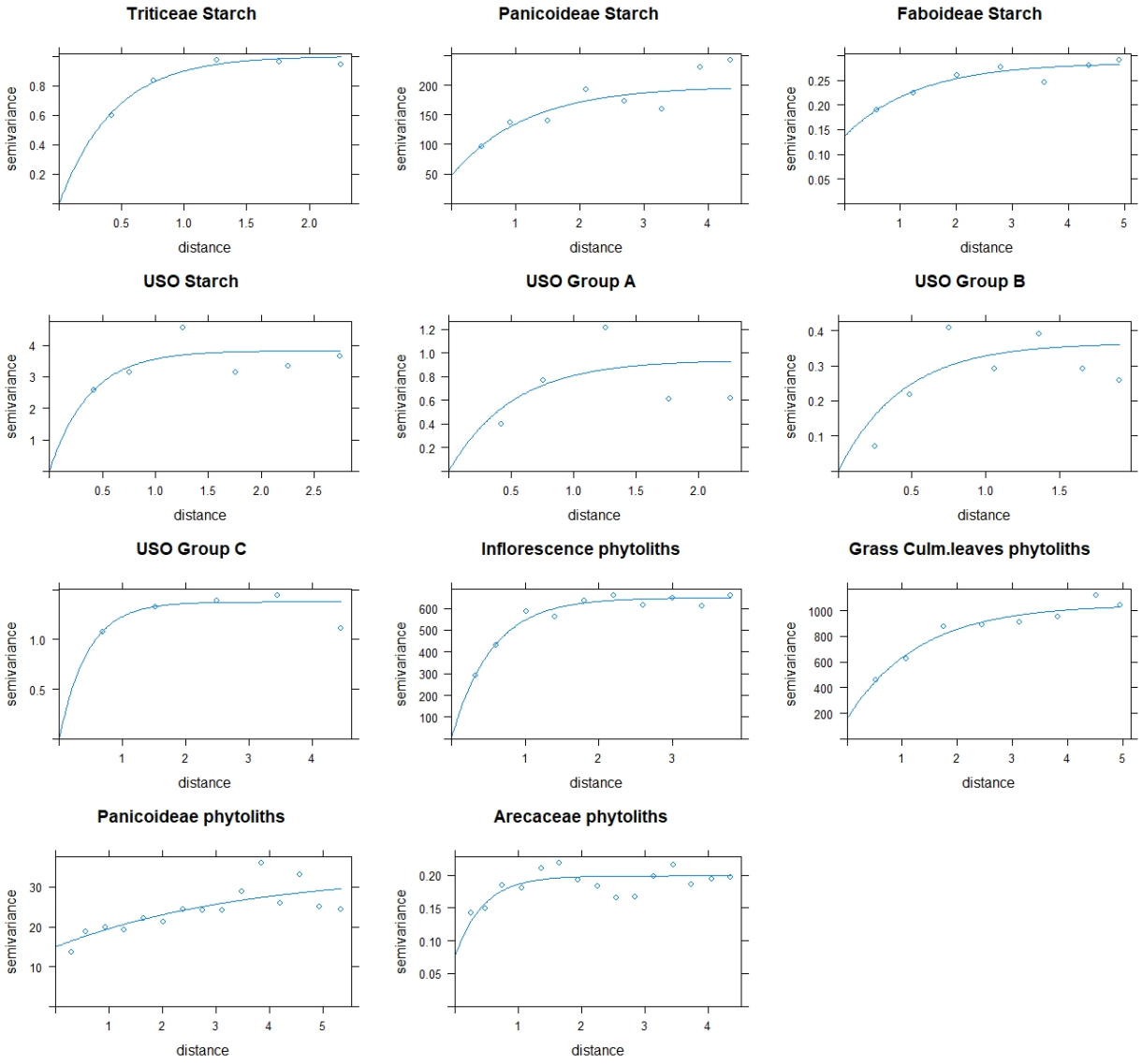

Figure S10. Fitted variograms for the ordinary kriging spatial analyses of starch grains and phytoliths from Building 80.

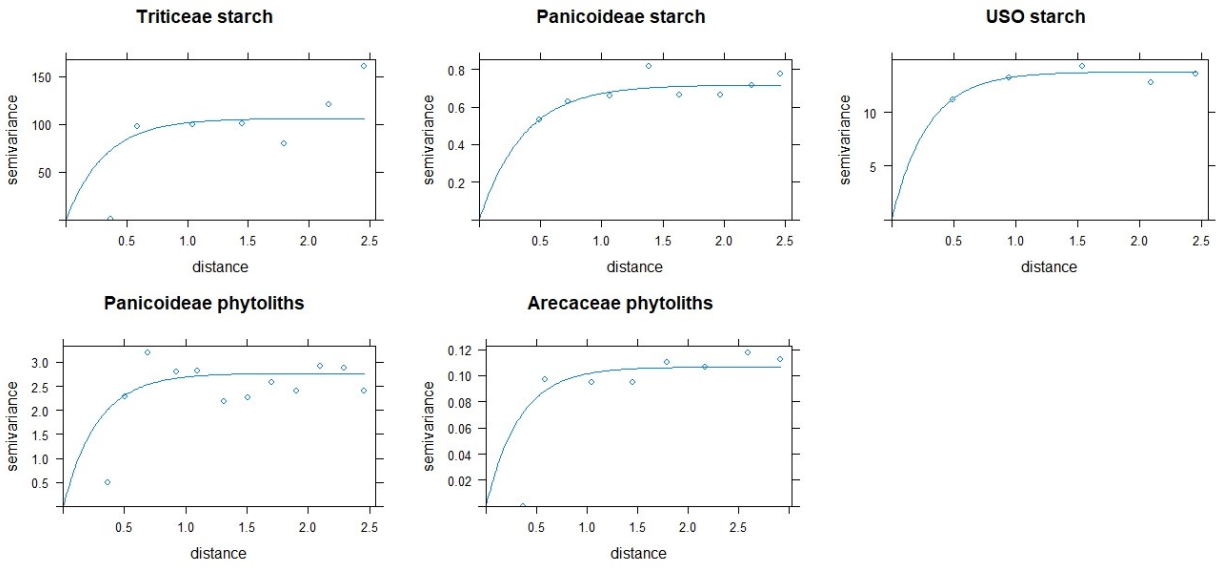

Figure S11. Fitted variograms for the ordinary kriging spatial analyses of starch grains and phytoliths from Building 131.

3.0 Ordinary kriging error variances

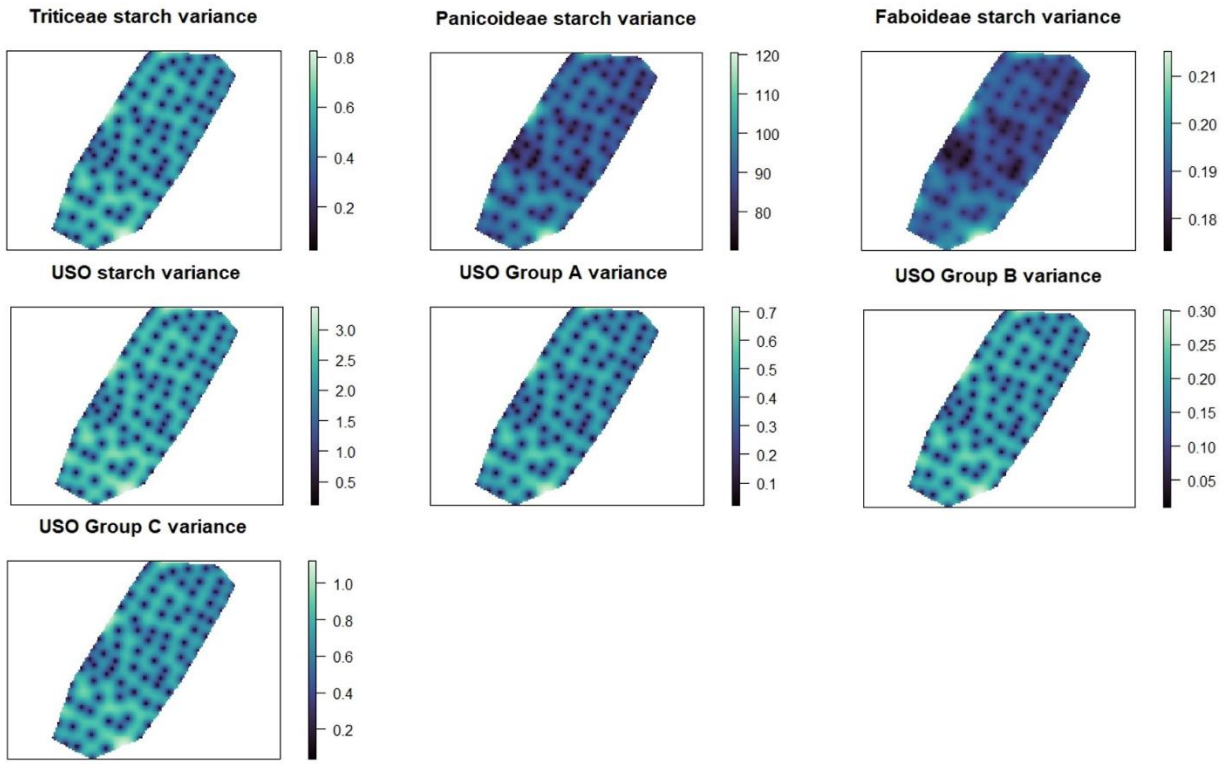

Figure S12. Ordinary kriging error variance for the interpolated starch grains categories from Building 80.

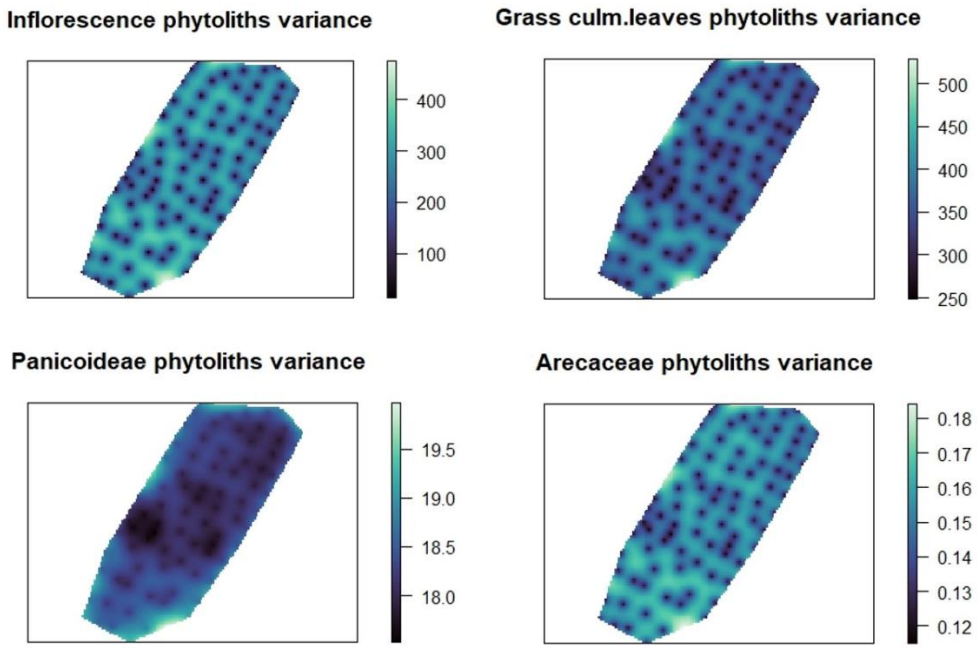

Figure S13. Ordinary kriging error variance for the interpolated phytoliths categories from Building 80.

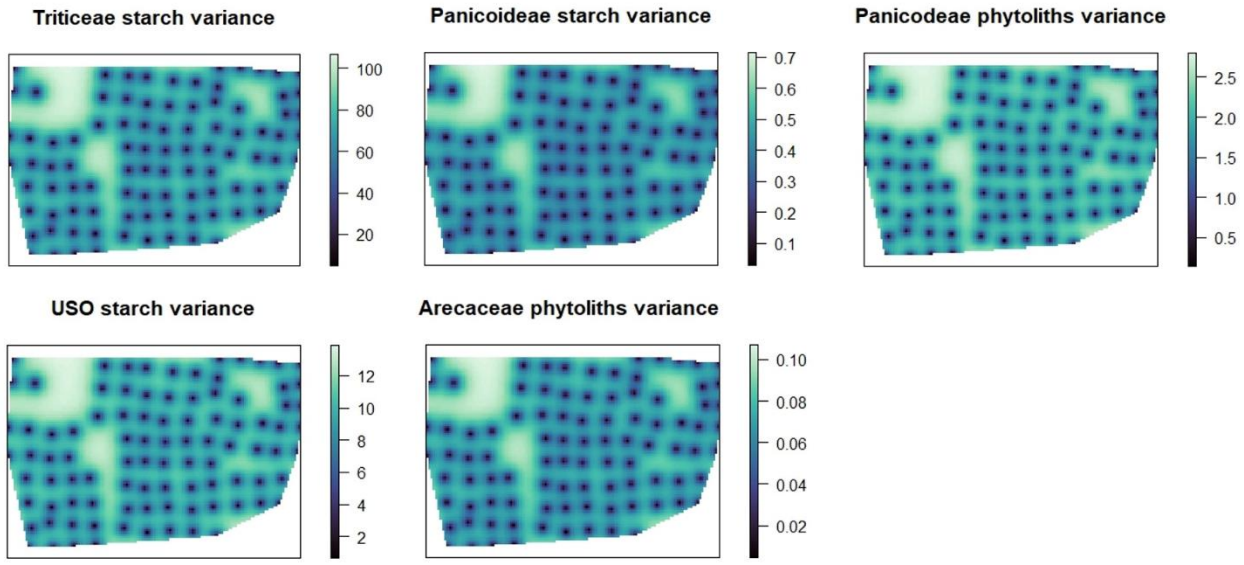

Figure S14. Ordinary kriging error variance for the interpolated phytoliths categories from Building 131.

References

Ahituv, H., Henry, A.G., 2022. Supplementary data - An initial key of starch grains from edible plants of the Eastern Mediterranean for use in identifying archaeological starches. Journal of Archaeological Science: Reports 42, 103396. https://doi.org/10.1016/j.jasrep.2022.103396

Ao, Z., Jane, J., 2007. Characterization and modeling of the A- and B-granule starches of wheat, triticale, and barley. Carbohydr. Polym 67, 46–55. https://doi.org/10.1016/j.carbpol.2006.04.013

Barton, H., Mutri, G., Hill, E., Farr, L., Barker, G., 2018. Use of grass seed resources c.31 ka by modern humans at the Haua Fteah cave, northeast Libya. J. Archaeol. Sci. 99, 99–111. https://doi.org/10.1016/j.jas.2018.08.013

Cagnato, C., Hamon, C., Salavert, A., Elliott, M., 2021. Supplementary materials - Developing a Reference Collection for Starch Grain Analysis in Early Neolithic Western Temperate Europe. Open Archaeology 7, 1035–1053. https://doi.org/10.1515/opar-2020-0186

Cristiani, E., Radini, A., Edinborough, M., Borić, D., 2016. Dental calculus reveals Mesolithic foragers in the Balkans consumed domesticated plant foods. PNAS 113, 10298–10303. https://doi.org/10.1073/pnas.1603477113

Cristiani, E., Zupancich, A., Duches, R., Carra, M., Caricola, I., Fontana, A., Flor, E., Fontana, F., 2021. Non-flaked stones used in the Mesolithic Eastern Alpine Region: A functional assessment from Romagnano Loc III and Pradestel sites. Journal of Archaeological Science: Reports 37, 102928. https://doi.org/10.1016/j.jasrep.2021.102928

Dubreuil, L., Savage, D., Delgado-Raack, S., Plisson, H., Stephenson, B., de la Torre, I., 2015. Current Analytical Frameworks for Studies of Use–Wear on Ground Stone Tools., in: Marreiros, J.M., Gibaja Bao, J.F., Ferreira Bicho, N. (Eds.), Use-Wear and Residue Analysis in Archaeology, Manuals in Archaeological Method, Theory and Technique. Springer, pp. 105–158. https://doi.org/10.1007/978-3-319-08257-8_7

García-Granero, J.J., Urem-Kotsou, D., Bogaard, A., Kotsos, S., 2018. Cooking plant foods in the northern Aegean: Microbotanical evidence from Neolithic Stavroupoli (Thessaloniki, Greece). Quat. Int. 496, 140–151. https://doi.org/10.1016/j.quaint.2017.04.007

Geera, B.P., Nelson, J.E., Souza, E., Huber, K.C., 2006. Composition and Properties of A- and B-type Starch Granules of Wild-Type, Partial Waxy, and Waxy Soft Wheat. Cereal Chemistry Journal 83, 551–557. https://doi.org/10.1094/CC-83-0551

Gott, B., Barton, H., Torrence, R., 2006. Biology of starch., in: Torrence, R., Barton, H. (Eds.), Ancient Starch Research. Left Coast Press., Walnut Creek, California, pp. 36–45.

Guan, Y., Pearsall, D.M., Gao, X., Chen, F., Pei, S., Zhou, Z., 2014. Plant use activities during the Upper Paleolithic in East Eurasia: Evidence from the Shuidonggou Site, Northwest China. Quaternary International 347, 74–83. https://doi.org/10.1016/j.quaint.2014.04.007

Haslam, M., 2004. The decomposition of starch grains in soils: implications for archaeological residue analyses. J. Archaeol. Sci. 31, 1715–1734. https://doi.org/10.1016/j.jas.2004.05.006

Henry, A., 2020. Starch Granules as Markers of Diet and Behavior., in: Henry, A.G. (Ed.), Handbook for the Analysis of Micro-Particles in Archaeological Samples, Interdisciplinary Contributions to Archaeology. Springer International Publishing, Cham, pp. 97–116. https://doi.org/10.1007/978-3-030-42622-4

Henry, A.G., Hudson, H.F., Piperno, D.R., 2009. Changes in starch grain morphologies from cooking. J. Archaeol. Sci. 36, 915–922. https://doi.org/10.1016/j.jas.2008.11.008
Lentfer, C., 2009. Building a comparative starch reference collection for Indonesia and its application to palaeoenvironmental and archaeological research, in: Haslam, M., Robertson, G., Crowther, A., Nugent, S., Kirkwood, L. (Eds.), Archaeological Science Under a Microscope: Studies in Residue and Ancient DNA Analysis in Honour of Thomas H. Loy. ANU Press. https://doi.org/10.22459/TA30.07.2009.07
Liu, L., 2015. A long process towards agriculture in the middle Yellow River Valley, China: Evidence from macro-and micro-botanical remains. JIPA 35, 3. https://doi.org/10.7152/jipa.v35i0.14727
Liu, L., Bestel, S., Shi, J., Song, Y., Chen, X., 2013. Paleolithic human exploitation of plant foods during the last glacial maximum in North China. Proceedings of the National Academy of Sciences 110, 5380–5385. https://doi.org/10.1073/pnas.1217864110
Liu, L., Duncan, N.A., Chen, X., Liu, G., Zhao, H., 2015. Plant domestication, cultivation, and foraging by the first farmers in early Neolithic Northeast China: Evidence from microbotanical remains. The Holocene 25, 1965–1978. https://doi.org/10.1177/0959683615596830
Liu, L., Kealhofer, L., Chen, X., Ji, P., 2014a. A broad-spectrum subsistence economy in Neolithic Inner Mongolia, China: Evidence from grinding stones. The Holocene 24, 726–742. https://doi.org/10.1177/0959683614526938
Liu, L., Levin, M.J., Bonomo, M.F., Wang, J., Shi, J., Chen, X., Han, J., Song, Y., 2018a. Harvesting and processing wild cereals in the Upper Palaeolithic Yellow River Valley, China. Antiquity 92, 603–619. https://doi.org/10.15184/aqy.2018.36
Liu, L., Li, Y., Hou, J., 2020. Making beer with malted cereals and qu starter in the Neolithic Yangshao culture, China. Journal of Archaeological Science: Reports 29, 102134. https://doi.org/10.1016/j.jasrep.2019.102134
Liu, L., Ma, S., Cui, J., 2014b. Identification of starch granules using a two-step identification method. J. Archaeol. Sci. 52, 421–427. https://doi.org/10.1016/j.jas.2014.09.008
Liu, L., Wang, J., Levin, M.J., Sinnott-Armstrong, N., Zhao, H., Zhao, Y., Shao, J., Di, N., Zhang, T., 2019. The origins of specialized pottery and diverse alcohol fermentation techniques in Early Neolithic China. PNAS 116, 12767–12774. https://doi.org/10.1073/pnas.1902668116
Liu, L., Wang, J., Rosenberg, D., Zhao, H., Lengyel, G., Nadel, D., 2018b. Fermented beverage and food storage in 13,000 y-old stone mortars at Raqefet Cave, Israel: Investigating Natufian ritual feasting. J. Archaeol. Sci. Rep 21, 783–793. https://doi.org/10.1016/j.jasrep.2018.08.008
Lucarini, G., Radini, A., 2020. First direct evidence of wild plant grinding process from the Holocene Sahara: Use-wear and plant micro-residue analysis on ground stone tools from the Farafra Oasis, Egypt. Quat. Int. 555, 66–84. https://doi.org/10.1016/j.quaint.2019.07.028
Lucarini, G., Radini, A., Barton, H., Barker, G., 2016. The exploitation of wild plants in Neolithic North Africa. Use-wear and residue analysis on non-knapped stone tools from the Haua Fteah cave, Cyrenaica, Libya. Quat. Int. 410, 77–92. https://doi.org/10.1016/j.quaint.2015.11.109

Madella, M., Lancelotti, C., García-Granero, J.J., 2016. Millet microremains—an alternative approach to understand cultivation and use of critical crops in Prehistory. Archaeol Anthropol Sci 8, 17–28. https://doi.org/10.1007/s12520-013-0130-y

Mercader, J., Abtosway, M., Bird, R., Bundala, M., Clarke, S., Favreau, J., Inwood, J.L., Itambu, M., Larter, F., Lee, P., Patalano, R., Soto, M., Tucker, L., Walde, D., 2018. Morphometrics of Starch Granules from Sub-Saharan Plants and the Taxonomic Identification of Ancient Starch. Front. Earth Sci. 6, 146. https://doi.org/10.3389/feart.2018.00146

Mickleburgh, H.L., Pagán-Jiménez, J.R., 2012. Supplementary material. Appendix A - Grinding experiment with modern maize landraces. New insights into the consumption of maize and other food plants in the pre-Columbian Caribbean from starch grains trapped in human dental calculus. Journal of Archaeological Science 39, 13. https://doi.org/10.1016/j.jas.2012.02.020

Pagán-Jiménez, J.R., 2015. Almidones: Guía de material comparativo moderno del Ecuador para los estudios paleoetnobotánicos en el Neotrópico. Instituto Nacional de Patrimonio Cultural, Quito, Ecuador.

Pfister, B., Zeeman, S.C., 2016. Formation of starch in plant cells. Cell. Mol. Life Sci. 73, 2781–2807. https://doi.org/10.1007/s00018-016-2250-x

Santiago-Marrero, C.G., Tsoraki, C., Lancelotti, C., Madella, M., 2021. A microbotanical and microwear perspective to plant processing activities and foodways at Neolithic Çatalhöyük. PLoS ONE 16, e0252312. https://doi.org/10.1371/journal.pone.0252312

Sugiyama, N., Sugiyama, S., Cagnato, C., France, C.A.M., Iriki, A., Hughes, K.S., Singleton, R.R., Thornton, E., Hofman, C.A., 2022. Earliest evidence of primate captivity and translocation supports gift diplomacy between Teotihuacan and the Maya. Proc. Natl. Acad. Sci. U.S.A. 119, e2212431119. https://doi.org/10.1073/pnas.2212431119

Torrence, R., 2006. Starch in Sediments, in: Torrence, R., Barton, H. (Eds.), Ancient Starch Research. Left Coast Press., Walnut Creek, California, pp. 145–176.

Tsafou, E., García-Granero, J.J., 2021. Beyond staple crops: exploring the use of 'invisible' plant ingredients in Minoan cuisine through starch grain analysis on ceramic vessels. Archaeol Anthropol Sci 13, 128. https://doi.org/10.1007/s12520-021-01375-4

Wang, J., Jiang, L., 2021a. Intensive acorn processing in the early Holocene of southern China. The Holocene 32, 1305–1316. https://doi.org/10.1177/09596836211041732

Wang, J., Jiang, L., 2021b. Supplemental material for Intensive acorn processing in the early Holocene of southern China. The Holocene. https://doi.org/10.1177/09596836211041732

Wang, J., Jiang, L., Sun, H., 2021. Early evidence for beer drinking in a 9000-year-old platform mound in southern China. PLoS ONE 16, e0255833. https://doi.org/10.1371/journal.pone.0255833

Wang, J., Liu, L., Georgescu, A., Le, V.V., Ota, M.H., Tang, S., Vanderbilt, M., 2017. Identifying ancient beer brewing through starch analysis: A methodology. J. Archaeol. Sci. Rep 15, 150–160. https://doi.org/10.1016/j.jasrep.2017.07.016

Wang, J., Zhao, X., Wang, H., Liu, L., 2019. Plant exploitation of the first farmers in Northwest China: Microbotanical evidence from Dadiwan. Quaternary International 529, 3–9. https://doi.org/10.1016/j.quaint.2018.10.019

Yang, X., Perry, L., 2013. Identification of ancient starch grains from the tribe Triticeae in the North China Plain. J. Archaeol. Sci. 40, 3170–3177. https://doi.org/10.1016/j.jas.2013.04.004

Yang, X., Zhang, J., Perry, L., Ma, Z., Wan, Z., Li, M., Diao, X., Lu, H., 2012. From the modern to the archaeological: starch grains from millets and their wild relatives in China. J. Archaeol. Sci. 39, 247–254. https://doi.org/10.1016/j.jas.2011.09.001

Yang, Y., Li, W., Yao, L., Cheng, Z., Luo, W., Zhang, J., Lin, L., Gan, H., Yan, L., 2016. Plant food sources and stone tools' function at the site of Shunshanji based on starch grain analysis. Sci. China Earth Sci. 59, 1574–1582. https://doi.org/10.1007/s11430-016-5321-9

Yao, L., Yang, Y., Sun, Y., Cui, Q., Zhang, J., Wang, H., 2016. Early Neolithic human exploitation and processing of plant foods in the Lower Yangtze River, China. Quaternary International 426, 56–64. https://doi.org/10.1016/j.quaint.2016.03.009

Zhang, N., Dong, G., Yang, X., Zuo, X., Kang, L., Ren, L., Liu, H., Li, H., Min, R., Liu, X., Zhang, D., Chen, F., 2017. Diet reconstructed from an analysis of plant microfossils in human dental calculus from the Bronze Age site of Shilinggang, southwestern China. J. Archaeol. Sci. 83, 41–48. https://doi.org/10.1016/j.jas.2017.06.010

Zhang, X., Zhu, X., Hu, Y., Zhou, Z., Olsen, J.W., Guan, Y., 2021. Ancient Starch Remains Reveal the Vegetal Diet of the Neolithic Late Dawenkou Culture in Jiangsu, East China. Front. Ecol. Evol. 9, 722103. https://doi.org/10.3389/fevo.2021.722103